Fuel 225 (2018) 287–298

Contents lists available at ScienceDirect

Fuel

journal homepage: www.elsevier.com/locate/fuel

Full Length Article

Ultrasound cavitation intensified amine functionalization: A feasible strategy for enhancing CO_2 capture capacity of biochar

Riya Chatterjee[a], Baharak Sajjadi[a,*], Daniell L. Mattern[b], Wei-Yin Chen[a], Tetiana Zubatiuk[c], Danuta Leszczynska[c], Jerzy Leszczynski[c], Nosa O. Egiebor[d,1], Nathan Hammer[b]

[a] Department of Chemical Engineering, School of Engineering, University of Mississippi, 134 Anderson Hall, MS 38677-1848, USA
[b] Department of Chemistry and Biochemistry, University of Mississippi, Coulter Hall, MS 38677, USA
[c] Interdisciplinary Center for Nanotoxicity, Jackson State University, 1400 J. R. Lynch Street, Jackson, MS 39217, USA
[d] Environmental Resources Engineering Department, College of Environmental Science and Forestry (ESF), 206 Bray Hall, Syracuse, NY 13210, USA

GRAPHICAL ABSTRACT

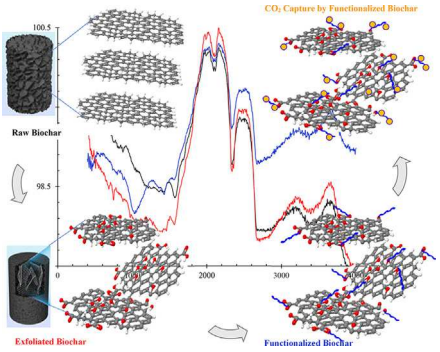

ARTICLE INFO

Keywords:
Biochar
Ultrasound
CO_2 capture
Tetraethylenepentamine (TEPA)
Amine functionalization
Adsorption

ABSTRACT

This paper describes a two-stage biochar activation process for CO_2 capture, which includes acoustic treatment and amination. Contrarily to traditional carbon activation at temperatures above 700 °C, both stages of the current process are conducted at or near room temperature. It is known that CO_2 can be fixed on the edge carbons of polycyclic aromatics hydrocarbons (PAHs) through thermal and reductive photo-carboxylation. Our previous work on biochar suggested that carbon of CO_2 could be chemically fixed on biochar through acoustic or photochemical treatment of biochar in water/CO_2 systems under ambient conditions. Separately, the graphene oxide (GO) literature reveals that carboxylic acids, epoxy and hydroxyl groups on biochar surface often serve as the active sites for converting GO to a new family of chemicals; amines are commonly grafted on these groups in the functionalization. Biochar has graphite and graphitic oxide clusters that consist of the oxygen functional groups mentioned above. These oxygen functionalities can be utilized for CO_2 adsorption when functionalized with amine. Thus, the present study focuses on maximizing the CO_2 capture capacity by manipulating the physicochemical structure of a pinewood-derived biochar. In this two-stage process, 30 s sonication at ambient temperature was applied to physically activate biochar prior to functionalization. Low-frequency ultrasound irradiation exfoliates and breaks apart the irregular graphitic layers of biochar, and creates new/opens the blocked microspores, thus enhancing the biochar's porosity and permeability that are the keys in functionalization and subsequent CO_2 capture. The sono-modified biochar was then functionalized with

* Corresponding author.
E-mail address: bsajjadi@olemiss.edu (B. Sajjadi).
[1] Formerly with Chemical Engineering Department, School of Engineering, University of Mississippi, 134 Anderson Hall, Oxford, MS 38677-1848, USA.

https://doi.org/10.1016/j.fuel.2018.03.145
Received 12 February 2018; Received in revised form 15 March 2018; Accepted 21 March 2018

tetraethylenepentamine (TEPA) in the presence of two activating agents. The changes in surface characteristics, functional groups, graphene-like structure, and functionalization using activating agents were examined in detail and the capacity of the final products in CO_2 removal was tested. The experimental results revealed that CO_2 capture capacity, from a flow containing 10 and 15 vol% CO_2, was almost 7 and 9 times higher, respectively, for ultrasound-treated amine-activated biochar, compared to raw biochar. The optimum capacity was 2.79 mmol/g at 70 °C and 0.15 atm CO_2 partial pressure. Cyclic adsorption and desorption tests revealed that the CO_2 capture capacity decreased 44% after 15 cycles.

1. Introduction

The boon of rapid industrialization has elevated standards of living but at the expense of environmental deterioration. During the span of a century, there has been an unprecedented increase in the level of greenhouse gases such as CO_2, CH_4, N_2O, etc., among which CO_2 plays a critical role in climate change and global warming. Increased anthropogenic activities such as flue gas emission from fossil-fuel fired power plants and industrial facilities has resulted in elevated concentration of carbon dioxide in the atmosphere. Statistics reveal that CO_2 contributes more than 60% to global warming [1]. The concentration of CO_2 in the atmosphere has increased 28% to its current value of 383 ppm, which is significantly higher than the pre-industrial level (300 ppm) [2]. It is estimated that between 2010 and 2060, fossil fuel combustion will emit 282–701 gigatons of CO_2, assuring the problems of climate change and global warming will continue [3]. Therefore, it has become imperative to develop Carbon Capture and Storage (CCS) technology to combat the global warming and climate change problem.

According to the most recent version (August 2015) of the Carbon Dioxide Capture Handbook published by the National Energy Technology Laboratory (NETL), the CO_2 capture technology can be divided into i) solvent based process (absorption), ii) sorbent based process (adsorption), and iii) membrane based process [4]. The above-mentioned processes can be applied both in pre-combustion CO_2 capture and post-combustion CO_2 capture. However, in this paper the focus is on post-combustion CO_2 capture. Different strategies of post-combustion (including absorption and adsorption) technique and their advantages/disadvantages are illustrated in Table 1. Another classification for CO_2 capture is based on the type of sorbent [2] used. Sorbent-based CO_2 capture involves primarily three types of adsorbents: i) inorganic adsorbents, ii) organic and organic-inorganic hybrids, and iii) metal organic frameworks. Inorganic adsorbents are further categorized as physisorbents (such as zeolites, activated carbon) and chemisorbents (such as metal-based and hydrotalcite-like compounds). Organic and organic-inorganic hybrid sorbents consist of amines supported on various oxides. Therefore, they can be grouped based on the type of support used. These include: i) amine physically adsorbed on oxide support, ii) amine covalently attached to oxide support, and iii) amine supported on solid organic materials.

As shown in Table 1, carbonaceous adsorbents are attractive for CO_2 sequestration. In recent years, biochar, which is derived from organic carbonaceous sources, has been gaining increasing attention as a carbon sequestration medium and potent soil amendment. Biochar is produced by pyrolysis that involves burning of (waste) biomass under oxygen-free conditions, which makes it less susceptible to degradation. It can also be derived as a byproduct during bio-oil production in inert atmosphere at elevated temperature. Biochar has a highly porous structure with a high surface area, and since it is produced from easily available, natural biomass it is an eco-friendly adsorbent. The abundance of feedstock source for biochar makes it almost ten times cheaper than other CO_2 adsorbents. Most importantly, biochar is stable, with an average carbon half-life for environmental oxidation of 100 to 10^7 years [5], depending on the amounts of aliphatic and volatile components. Due to its potentially large storage capacity when mixed in soil, it has been considered as a major carbon storage method for mitigating climate change [6]. Aslanzadeh et al. [7] reported that up to 12% of anthropogenic CO_2 emissions can be reduced by the storage of biochar in soil. Creamer et al. [3] conducted CO_2 capture experiments using two types of biochar produced from sugarcane bagasse and hickory wood feedstocks and could achieve CO_2 adsorption capacity of around 1.67 mmol/g for sugarcane bagasse-based biochar at 25 °C [3]. Therefore, it is reasonable to say biochar is a potential adsorbent of CO_2, but the adsorption capacity of raw biochar is not very high. Hence, to maximize the CO_2 capture capacity, surface modification is required. This can include both physical modification and chemical modification.

Biochar structure consists of graphite clusters that contain graphene oxide (GO) layers. The graphene oxide layers have reactive oxygen functional groups such as carboxyl, epoxy, and hydroxyl. However, these oxygen functionalities are accessible only for exfoliated biochar. Biochar is produced at elevated temperature, and its pristine graphitic oxide structure prevents any interaction, so that the graphene oxide layers remain inaccessible. But exfoliated biochar has oxygen functionalities available for further interaction. Interaction or activation with appropriate basic functional groups such as amine is desired due to the following reasons [8]. The carbon atom in CO_2 is electrophilic (electron deficient) because of the high electron negativity of the oxygen atoms. Amines are nucleophilic because of the presence of a lone pair of electrons and therefore can interact with CO_2. Thus, the amine-modified biochar has improved adsorption capacity compared to raw char. On the other hand, the graphitic cluster (basic structure of biochar) tends to agglomerate in the presence of water, blocking the pores that are active sites for CO_2 adsorption. This reduces the adsorption capacity by reducing the specific surface area. To overcome this problem, biochar needs to be mixed homogeneously into the water. Ultrasonic irradiation can prevent the formation of an agglomerated graphitic sheet by exfoliation of biochar.

Previous work of our research group [6] suggested that reductive photo-carboxylation of biochar's polyaromatic hydrocarbons (PAH) edge carbons enhances its hydrogen content (up to 24%) and that in turn increases its energy content (up to 50%). The work also demonstrated that biochar was exfoliated into graphitic and graphene oxide clusters in the CO_2 + H_2O system under ultrasound irradiation and this facilitated the reactivity of edge carbons of these platelets. The presence of CO_2 favors the ability of PAH to capture and convert CO_2 to carboxylic acid products, as demonstrated by Chateauneuf et al. [9]. Biochar with exfoliated basic graphene oxide clusters is expected to be more susceptible to chemical modification since more surface is available for modification. In other words, the improvement of biochar structure can be further boosted by irradiation under low-frequency ultrasound. Moreover, the cavitation effect of ultrasound makes a uniform biochar suspension, activates the binding sites, and leads to better grafting of functional groups. A similar trend was observed in work conducted by Park et al. [10] where ultrasound facilitated the preparation of a homogeneous colloidal suspension of polyanilineamine (PAA)-modified graphene oxide sheets. Previous work by our research group formed the basis of our current study and served as a motivation for economically modifying and functionalizing biochar with amine groups and utilizing it as a potent CO_2 adsorbent. To achieve this goal, the carbonaceous structure of biochar was improved both physically under ultrasound irradiation and chemically through amine functionalization. The effectiveness of physicochemical-activated (ultrasound treated-amine functionalized) biochar was determined by comparison

Table 1
Different absorption and adsorption strategies for CO_2 capture.

Advantages	Efficiency	Disadvantages	Cost effectiveness	Ref
Absorption				
1. Physical absorption ● SP – low vapor pressure, toxicity, less corrosive solvent ● RP – solvent is less corrosive and more stable ● PP – low energy consumption ● MP – easy to operate ● FP – used to remove high concentration CO_2	85% of the CO_2 from flue gas can be captured efficiently	- Needs high pressure 2.07–13.8 MPa - Solvent disposal is a problem - Reaction of solvents with constituent - Operating temperature is very low	Because of high pressure and low temperature, the process is not cost effective	[1], [33]
2. Chemical absorption ● **Amine absorption** - Since CO_2 reacts chemically with amine, it can be used to process gas streams with low CO_2 partial pressure	CO_2 removal: 0.4 kg CO_2/kg monoethanol amine	- Solvent regeneration not fully achieved - Energy intensive process - Waste stream can be hazardous	Not economic: i) Not complete solvent regeneration ii) high energy demand	[34]
● **Aqua ammonia absorption** - Used for multi pollutant removal - Equipment corrosion negligible - No degradation of absorbent - Byproducts (NH_4NO_3 & sulfate) used as fertilizer	CO_2 removal: 1.20 kg CO_2/kg ammonia is satisfactory	- Flue gas must be cooled to 15–27 °C due to volatility of ammonia - Solids formation upon CO_2 capture; equipment plugging - Ammonia vapor losses during stripping	Not economically attractive because energy lose during the cooling of feed	[34]
● **Dual alkali absorption** - Better replacement of the Solvay process - Absorption capacity better than amine process	CO_2 removal: 0.54 kg CO_2/kg methylaminoethanol	- Gas stream must be cooled to 25 °C - Removal of NOx-SOx prior to absorption - Solvent regeneration not yet achieved	Solvent regeneration is not possible to achieve-not cost effective	[34]
Absorption with carbonate slurry- Useful for multi pollutant capture using non-hazardous and non-volatile Na_2CO_3 solvent	CO_2 removal: 0.73 kg CO_2/kg CO_3^{2-}	- Slow absorption rate - Required tall absorption columns +	High operating cost and slower rate economically unattractive	[34]
● **Ionic liquid** - Applied either physically or chemically - Low vapor pressure, good thermal stability, high polarity, and non-toxicity - Chemical absorption of IL is higher than physical one	CO_2 removal: 0.20 mol of CO_2 per mole of IL	-ILs are highly viscous thus needed blended solution with alkanolamine - Supported ILs to improve efficiency of the process	Not economic because of low absorption rate and use of blended solution	[34]
Adsorption				
1) **Traditional adsorbents** ● **Carbonaceous adsorbents** - High thermal stability; favorable adsorption kinetics - Cheaper feedstock sources - Desorption is accomplished by the pressure swing approach	CO_2 adsorption: 0.1–1.13 g CO_2/g activated carbon	- Unable to treat high pressure gases - Needs separate characterizations depending feedstock - Adsorption rate reduces when exposed to NOx, SOx & H_2O	The CO_2 capture costs are such that the carbon-based systems can be applicable when CO_2 purity is not more than 90%	[34]
● **Zeolites** - CO_2/N_2 selectivity is much higher than activated carbon - Enhanced capacity and selectivity than physical sorbents	CO_2 adsorption: 0.004 to 0.216 g CO_2/g zeolite	- Efficiency reduces in presence of H_2O -Regeneration temperature high (> 300 °C) - Needs chemical modification	The high regeneration temperature makes the process less cost effective	[34]
● **Mesoporous silica** - High surface area; high pore volume - Tunable pore size - Good thermal and mechanical stability	Adsorption capacity is not sufficient	-Adsorption capacity not good at atmospheric pressure - Silica has lower adsorption capacity and selectivity toward CO_2	Low adsorption capacity makes the process less economic	[34]
● **Metal organic frameworks** - High thermal stability; high surface area - Adjustable chemical functionality - High adsorption capacity at elevated pressure - Easily tunable pore characteristics	CO_2 adsorption: 1.13 g CO_2/g adsorbent	- Adsorption capacities reduce in exposure to a gas mixture of NOx, SOx, and H_2O - Low CO_2 selectivity in CO_2/N_2 gas streams and PS and TS have not been thoroughly understood	Due to low sorbent regeneration, the technique is not cost effective	[34]
2) **Advanced adsorbents** ● **Fly-ash carbon enriched by 3-chloropropylamine-hydrochloride**	CO_2 adsorption: 174.6 μmol/g	- Needs chemical modification	Not cost effective	[4]
● **Modified mesocellular silica foams impregnated with tetraethylenepentamine (TEPA)**	CO_2 adsorption: 26.4–193.6 mg/g	- Adsorption capacity very low	Not cost effective	[35]
● **Amine functionalized adsorbents** - CO_2 partial pressure does not affect adsorption capacity - Moisture facilitates adsorption; favorable kinetics	CO_2 adsorption: 0.089–1.1 mmol/g adsorbent	- Degrade at temperatures around 100 °C - Irreversible reactions with NOx-SOx - Loss in capacity after desorption	The process not fully economic for large scale operation	[34]
● **Biochar**	CO_2 adsorption:1.67 mmol/g	- Surface functionalization may be required	Cost effective and viable	[3]

Note: **SP: Selexol Process**/Solvent: dimethylether or propylene glycol**, RP: Rectisol Process**/Solvent: Methanol**, PP: Purisol Process**/Solvent: N-methylpyrrolidone, **MP: Morphysorb Process**/Solvent: Morpholine**, FP: Fluor Process**/ Solvent: Propylene Carbonate, **PS:** Pressure swing, **TS:** temperature swing.

with: I) raw biochar, and II) currently available commercial or modified CO_2 adsorbents.

2. Materials and methods

2.1. Materials

Raw biochar was supplied by Biochar Now (Berthoud Colorado, U.S.A.). The feedstock used for this biochar is pine (soft wood biomass). The biomass is pyrolyzed (heated in oxygen-deprived environment) at elevated temperature (between 550 and 600 °C) in a kiln reactor with a multi-zone combustion chamber. After pyrolysis, the biochar is exposed to nitrogen to stop the process. The raw biochar pieces are too large for practical use, so they are resized at crushing and screening sections. Biochar with a size range of 26–50 mesh was selected for our present work and was further ground and sieved before activation.

The reagents used in chemical functionalization were methanol, N-(3-dimethylaminopropyl-N′-ethylcarbodiimide hydrochloride (EDC 98% purity), hydroxybenzotriazole (HOBt, 97% purity), and tetraethylenepentamine (TEPA), which were obtained from Sigma Aldrich. The chemicals used in filtration were hydrochloric acid (37%) from Sigma-Aldrich, deionized water, sodium hydroxide from Fisher Scientific, and acetone from Sigma-Aldrich. All chemicals used were of analytical grade.

2.2. Experimental method

2.2.1. Functionalization and ultrasound treatment of biochar

Before modification, biochar was sieved using Tyler standard screens; a particle size of range 75–106 μm was selected. Physical modification of biochar was achieved under 20 kHz low power ultrasound irradiation (Sonicator model No. XL2010 with maximum power of 475 W) and high-power ultrasound irradiation (QSonica sonicator model No. Q700 with maximum power of 700 W). The specified amount of raw biochar was treated under different ultrasound irradiation durations (30 s, 1, and 3 min). The ultrasonically-modified biochar was then subjected to chemical activation consisting of two steps. In the first step, the potential functional groups of biochar were activated with the activating agents EDC and HOBt in three different ratios (0.75:1, 1:1, and 1:0.75) in water. The mixture was stirred for 24 h at 35 °C, then filtered and dried under vacuum at 60 °C overnight. In the second step, the dried sample was suspended in methanol and amine (TEPA) was added in an amount ranging from 2.5 times to 15 times the weight of the activated biochar. The mixture was stirred for 24 h with gentle heating as before. Then it was cooled to room temperature, filtered with repeated washing first with 1 N NaOH, then with 1 N HCl, and finally with acetone, dried as before, and stored in a desiccator.

The physico-chemically modified biochar was characterized using Raman (LabRam HR Evolution) and Fourier Transform Infrared (FTIR, Cary 660 FTIR Agilent) spectroscopies to determine the surface functional groups and chemical species. The elemental compositions of biochar samples were analyzed before and after physico-chemical modification (Huffman Hazen Laboratory, Colorado, USA). The effects of ultrasound activation on micro and macro surface area and porosity were investigated by surface analyzer (Quantachrome 2000E series). Surface morphology of both raw and activated biochar was examined using SEM (JSM-5600 Scanning Electron Microscope, JEOL USA Inc., Peabody, MS).

2.3. CO_2 adsorption study

Adsorption experiments were conducted in a tubular reactor made of alumina oxide (Al_2O_3) of 12 cm length and 1.5 cm inner diameter. The adsorption column, containing 2 g of the functionalized biochar, was placed into a temperature-controlled furnace. CO_2 was diluted with helium gas (99.99%) at a flowrate of 500 $cm^3\,min^{-1}$ at 378 K for 1 h, and then cooled to 333 K. The helium flow was then switched to a CO_2-containing simulated flue gas of 10 vol% at a flow rate of 500 $cm^3\,min^{-1}$. The final concentration of CO_2 after adsorption was measured by a CO_2 analyzer, connected on-line via the adsorption column outlet. The adsorption capacity of CO_2 after a certain time was then calculated using the following equation:

$$q_a = \frac{1}{M} \times \left[\int_0^t Q \times (C_0 - C)\,dt \right] \times \frac{1}{V_m} \quad (1)$$

where, q_a is the adsorption capacity for CO_2, mmol/g; M is the mass of adsorbent, g; Q is the gas flow rate, $cm^3\,min^{-1}$; C_0 and C are influent and effluent CO_2 concentrations, vol%; t denotes the time, min; and V_m is 22.4 mL $mmol^{-1}$.

3. Results and discussions

3.1. Physical activation of biochar

Cavitation under ultrasound consists of 3 steps: nucleation, growing of bubbles, and finally collapse of bubbles with high energy and pressure. High energy increases temperature, and high pressure produces microjets within the liquid. These phenomena in the biochar-water mixture lead to chemical excitation of the biochar during which the materials inside the porous structure of biochar leach out, creating empty pores [6]. The empty pores then act as active sites for either

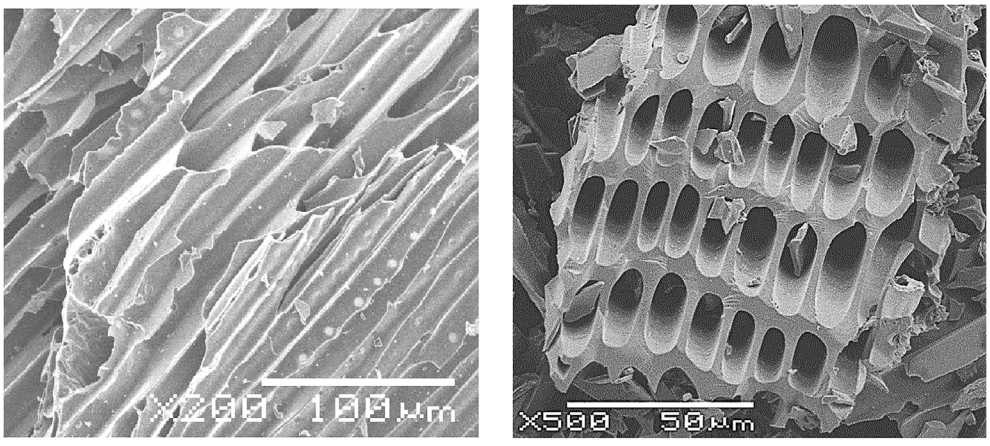

Fig. 1. SEM images of raw biochar. a) Longitudinal view, b) Cross-sectional view.

adsorption or chemical functionalization (with particular focus on amine groups in this study). Effectiveness of sonication in this study was initially investigated by comparing SEM images of raw and sonicated biochar as shown in Figs. 1 and 2, respectively. From both longitudinal view in Fig. 1a and cross-sectional view in Fig. 1b, it can be clearly seen the pores were blocked. Therefore, the structure remained inaccessible for modification. In traditional activating processes, a secondary pyrolysis, or a thermal treatment with high temperature (very energy consuming) are usually used for surface and structural modification. In this study it has been shown that sonication can play a pivotal role to clear the blockage. It can be proposed that micro-jets formed during sonication impinged with and penetrated through the biochar surface, thus clearing the pores. The results related to the effect of ultrasound irradiation on biochar structure are shown in Fig. 2a. The figure clearly portrays that the pores were exposed due to sonication. This helped in linking amine to the biochar in the subsequent functionalization step.

Ultrasound also aided in enhancing surface area, as shown in Table 2. As summarized in the table, the surface area and porosity changed with sonication for both micropores (described by DR-CO_2) and macropores (described by BET-N_2). Raw biochar's microporous surface area of 312.31 m^2/g increased to 354 m^2/g after 30 s of sonication. In contrast, the macroporous surface area reduced from 13.30 m^2/g for raw biochar to 10.13 m^2/g for 30 s sonicated biochar. The micropore behavior can be explained as an effect of microjet formation during cavitation. These micro-jects impinge on the surface and create more micropores, thus enhancing the microporous surface area. However, upon further increase of sonication duration to 1 min, the microporous surface area reduced to 268.82 m^2/g. This demonstrated that cavitation negatively affected the biochar structure at longer durations. As sonication time increased, cavitation intensity increased, and intensified cavitation disarranged the orientation of the layered structure of biochar, consequently blocking the pores and reducing adsorption capacity. Similar phenomena were observed by Verma et al. [11] and Hamdaoui et al. [12] where, in both cases, very high sonication times reduced the surface area, cumulatively reducing adsorption capacity. The high-pressure acoustic waves could further break the particles into smaller ones. These particles agglomerate and block pores, thus reducing the surface area. Particularly, low frequency ultrasound (20–100 kHz) induces particle size reduction, efficient mixing, and mass transport through cavitation [13].

Literature suggests that graphene oxide can be completely exfoliated under ultrasound irradiation, producing single-layer GO [14]. Since biochar has structural similarity with graphene oxide, it was expected to behave similarly under ultrasound irradiation, as discussed in the subsequent Raman analysis section. This exfoliation would facilitate the attack of edge carbons during amine functionalization of biochar. The novelty of the present work lies in using ultrasonic exfoliation to physically activate biochar. Other exfoliation techniques include the use of surfactants, strong acids, or other chemical reagents [15]. Using chemical agents for exfoliation increases the risk of toxicity and chemical hazard and leads to waste disposal problems; such treatment also consumes a high amount of energy if it is applied at elevated temperature. Therefore, sonication provides an easy, environmental friendly, economical and promising method of exfoliation.

3.2. Mechanism of chemical activation of biochar

The treatment of biochar with amines leads to amination that results in elevated adsorption capacity. The amine functionalization can take place in two ways where amine can replace oxygen functionalities of biochar. The first mechanism is conversion of a −COOH (carboxyl) group, the most suitable group for amination located at edge carbon, to a −CONHR (amide) group, where R contains an amine group. First of all, the carboxyl group must be chemically activated in order to react with an amine. The second mechanism is attachment of amine by ring opening of an epoxide group, which can occur without the aid of any activating agents. For last few decades, EDC-benzotriazole based coupling has provided efficient activation of carboxyl groups. The reagents and the EDC-benzotriazole by-products are water soluble. The basic chemistry of the amination reaction is depicted in Fig. 3. In step 1 and step 2 of Fig. 3 the reaction mechanism of the −COOH group with EDC-HOBT-TEPA is shown, and in step 3 the reaction of the epoxy group with amine is presented.

As shown in step 1, the coupling agent (EDC) activates the carboxylic acid group to form O-acylisourea as an intermediate. This intermediate could be displaced by nucleophilic attack from amino groups in the reaction mixture, producing amide and releasing iso-urea as a byproduct [16]. Another side reaction could be O—N migration of the activated carboxyl functional group forming an N-acyl urea [16]. Incorporation of appropriate additives prevents these side reactions and enhances the yield [16]. HOBt is a widely-used additive that prevents urea formation very effectively [17]. Besides, isolation of products from unreacted reagents can be done by simple filtration since urea is soluble in water [18]. Therefore, the chemical activation in this study incorporates HOBt as shown in Fig. 3. In Step 2 the amination of the activated carboxyl group by TEPA is shown. The second mechanism involves interaction of epoxy group with TEPA (Fig. 3, Step 3). However, in the presence of coupling agents, the former reaction is much faster than the latter one.

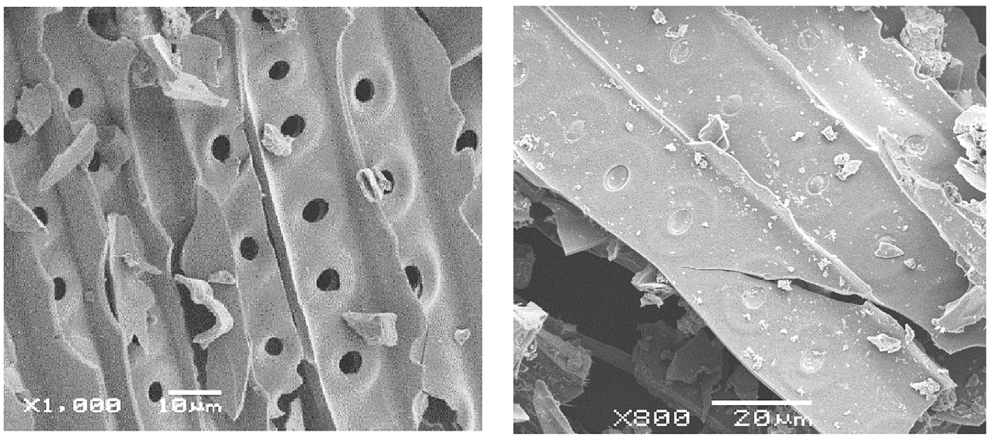

Fig. 2. SEM image of a) physically activated biochar under ultrasound irradiation of 20 kHz for 30 s, b) physio-chemically activated biochar after both ultrasound irradiation and amine functionalization.

Table 2
DR-CO_2 and BET-N_2 surface area of raw biochar, only ultrasound treated, and ultrasound treated-amine modified biochar.

Sample name	Micro-porosity			Macro & meso porosity		
	Surface area (m^2/g)	Pore volume (cm^3/g)	Pore Radius (nm)	Surface area (m^2/g)	Pore volume (cm^3/g)	Pore radius (nm)
Raw Biochar	312.31	0.11	0.60	13.30	0.005	0.80
US0.5-EH0-T0	354.37	0.12	0.58	10.13	0.01	2.30
US1.0-EH0-T0	268.82	0.09	0.62	18.15	0.02	1.30
US0.5-EH1:1-T2.5	261.68	0.09	0.63	9.39	0.02	4.80

Note: US: Ultrasound; EH: EDC-HOBt; T: TEPA. Number beside US denotes sonication time in minutes; Number beside EH denotes ratio of activating agents; Number beside T denotes amine loading.

3.2.1. Effect of physicochemical activation on elemental composition of biochar

The effects of chemical activating agents and ultrasonication on the amination of biochar by the amine TEPA were shown by elemental analysis of the organic elements C, N, O and S, as well as a determination of the ash content (Table 3). Since the ash content varied widely the elemental composition of the organic material alone was also calculated, omitting the contribution of ash; this is shown in Table 3A of the Supplementary Materials. Finally, it can be noted that the %C and % O of these samples varied in a way that suggested differing amounts of absorption of CO_2 by the samples. This nature of this absorption will be explored in a future study; for now, the compositions, under the assumption that any oxygen in the final samples above the amount in raw biochar came from absorbed CO_2 has been also calculated. These compositions, which omit the contributions resulting from absorbed CO_2, are displayed in Table 3B of the Supplementary Materials.

The activating reagents for amination, EDC and HOBt, were successful in promoting grafting of amine onto biochar whenever they were employed, as shown by the %N analyses in Table 3. The %N increased from 3 to 8 times its initial value in raw biochar. In contrast, and as expected, the use of ultrasound alone (entry 3) showed no significant increase in %N. The effectiveness of ultrasound in promoting chemical amination reactions gave inconsistent results, with no clear trends. For example, the use of 30 s of low-energy ultrasound (entry 4) gave the highest %N incorporation, but similar treatment with high-energy ultrasound (entry 7) gave the lowest.

In entries 4–6 and 7–9, we compare the effects on amination of exposure duration (0.5, 1, or 3 min) to low-power and high-power ultrasound, respectively. There were no significant differences in %N seen within these series, although the average incorporation of nitrogen seems somewhat higher under low-power ultrasound (1.09%) than high-power (0.59%).

The effect of using one of the two activating reagents in excess was also examined (entries 10–12); there was no significant change in the amount of nitrogen grafted into the biochar structure whether the ratio of activating agents, EDC:HOBt, was 1:0.75, 1:1, or 0.75:1. The effect of increasing the loading of the amine TEPA from a relative mass of 2.5 (entry 6) to 10 (entry 11) to 15 (entry 13) was investigated, all under 3 min of low-power ultrasound. As expected, the %N incorporation increased as the loading increased, consistent with the literature [19].

All treatments lowered the amount of sulfur in the biochar, from 0.05% to ≤0.02%. Ultrasound and amination had similar effects, and there was no apparent advantage to using both. This suggests that ultrasound could help lead to the production of sulfur-free, cleaner fuel.

Finally, the residual ash in the treated biochars was also examined, which varied widely. Three min of low-power ultrasound lowered the ash content from 23.95% (entry 1) to 19.43% (entry 3). The turbulence created by ultrasound enhances mass transfer and promotes the efficient leaching of minerals such as Ca, Mg and P [20]. However, the chemical amination procedure alone lowered the% ash even further, to 18.86% (entry 2). All but one of the combination treatments were more effective in lowering ash than ultrasound or chemical activation alone. There were no obvious trends, but there was a suggestion, contrary to expectations, that shorter ultrasound durations (e.g., entry 7) were more effective than longer ones (entry 9). This will be an area of further study.

Reduction of ash content is important in increasing the heating value of biochar, but these amination experiments are directed towards CO_2 capture; amination would not be a cost-effective way to add fuel to biochar. It can also be noted that as the %N increases due to the incorporation of TEPA, the %C of samples will decrease and the %H will increase, in the direction of the composition of TEPA. These consequences are seen most clearly in Table 3B, and do not indicate a change in the underlying structure of the biochar. Table 3B also shows no significant change in the %C of biochar due to sonication alone (entry 3).

3.2.2. Effect of physiochemical activation on functional groups of biochar

The results of FTIR spectroscopy of raw (R) and functionalized biochar with ultrasonic and chemical activation (US3-EH1:1-T10) and with ultrasonic activation alone (US3-EH0-T0), are depicted in Fig. 4. FTIR helps in identifying major functional groups that take part in activation. The overall FT-IR spectrum shape is similar for all the biochar samples. The IR spectrum of R was consistent with the presence of −COOH/−OH and C═O groups at 3400 and 1600 cm^{-1} respectively. A new peak in US3-EH1:1-T10 at 1000 cm^{-1} could be attributed to the vibration absorption of C−N of the incorporated amines. A strong peak around 3400 cm^{-1} was seen for OH stretching in US3-EH0-T0; amine N−H stretch around 3400 cm^{-1} was not distinguishable from O−H stretch.

The IR spectra of R, US3-EH1:1-T2.5, US3-EH1:1-T5, US3-EH1:1-T10 and US3-EH0-T0 are shown in Fig. 5. The peak around 1000 cm^{-1} which could be attributed to the vibration of C−N becomes more intense as the amine loading is increased from 2.5 to 10. A peak at 1423 cm^{-1} is not found for either R or US3-EH0-T0, but appeared in all amine activated samples; it is attributed to CH_2 bending vibrations introduced by the TEPA structure [21].

The efficacy of amine as a functionalizing agent was further demonstrated from the SEM image shown in Fig. 2b. The reaction with amine was facilitated due to the presence of pores. The SEM image portrayed that the porous structure as well as the surface were covered with amine.

3.2.3. Effect of physiochemical activation on graphitic structure of biochar

Raman spectroscopy provides useful information for characterizing carbonaceous compounds including graphitic oxide. Biochar has structural similarity with graphene oxide. So, Raman spectroscopic analysis is a useful tool for describing important characteristics of raw and modified biochar samples under different conditions. The Raman spectra for raw biochar (R) and biochar activated with different activating agent ratios (US3-EH1:1-T10, US3-EH1:0.75-T10, US3-EH0.75:1-T10) are shown in Fig. 6. Sonication duration and amine concentration for all the samples were the same; they differed in the ratios of chemical activators. For the Raman spectrum of raw biochar, a

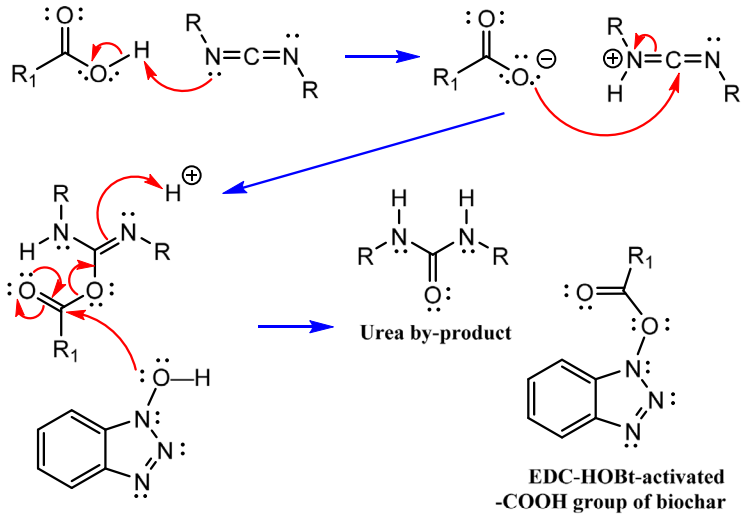

Step 1. Mechanism of EDC-HOBt coupling with –COOH group of biochar

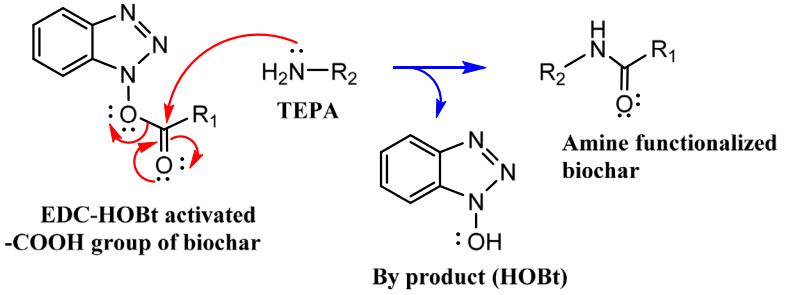

Step 2. Mechanism of TEPA functionalization of activated carbonyl group of biochar

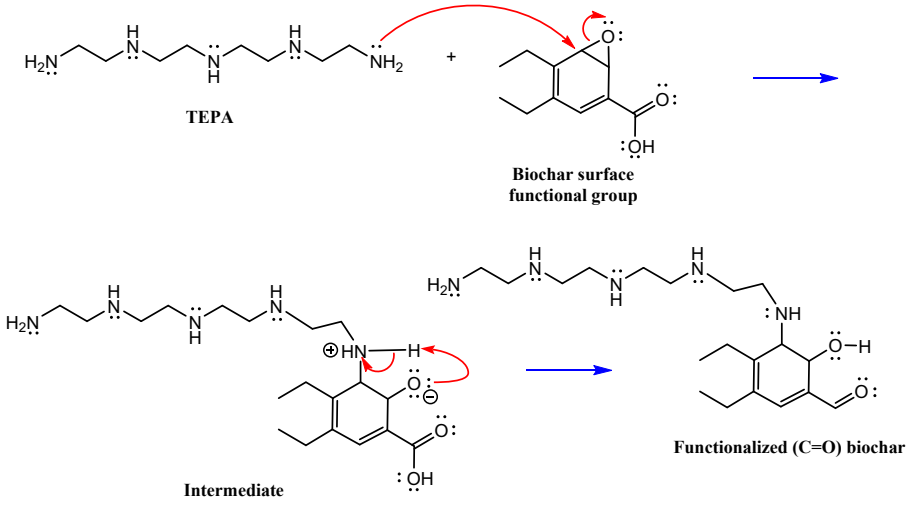

Step 3. Mechanism of TEPA functionalization of epoxy group of biochar

Fig. 3. EDC-HOBt coupling reaction and subsequent amine functionalization of biochar.

strong peak is observed in the range 2500–2800 cm^{-1}. This confirms the structural similarity of biochar and graphene oxide, since this peak is a signature peak of graphitic sp^2 structure [22]. The characteristic D band is observed at 1394 cm^{-1}, 1356 cm^{-1}, 1366 cm^{-1}, 1382 cm^{-1} for R, US3-EH1:1-T10, US3-EH0.75:1-T10 and US3-EH1:0.75-T10, respectively. The broader D band of raw biochar also signifies the presence of oxygen functional groups that lead to reduced size of the sp^2 domain of biochar by creating defects and distortions [22]. The characteristic G band, due to C–C bond stretch, is located at 1606 cm^{-1}, 1590 cm^{-1}, 1625 cm^{-1} and 1605 cm^{-1} for R, US3-EH1:1-T10, US3-EH0.75:1-T10 and US3-EH1:0.75-T10 respectively. Disorder of the sp^2 crystal structure can be determined from the intensity ratio between the D and G bands (I_D/I_G) [23]. The I_D/I_G ratio for raw biochar was 0.82; this value increased to 0.87 and 0.85 for 1:1 and 1:0.75 respectively, and reduced

Table 3
Elemental analysis of raw biochar and physico-chemical activated biochar.

Entry	Sample name	Ultrasound power	Ultrasound duration (min)	EDC:HOBt:TEPA wt:wt:wt	Carbon content (%w/w)	Hydrogen content (% w/w)	Nitrogen content (% w/w)	Oxygen content (% w/w)	Sulfur content (% w/w)	Ash content (% w/w)
1	Raw Biochar	–	–	–	65.36	1.97	0.18	11.22	0.05	23.95
2	US0-EH1:1-T2.5	–	–	1:1:2.5	62.21	2.31	0.93	15.24	0.02	18.86
3	US3-EH0-T0	Low	3	–	62.62	2.32	0.24	15.56	0.02	19.43
4	US0.5-EH1:1-T2.5	Low	0.5	1:1:2.5	69.61	2.61	1.63	11.36	0.02	13.93
5	US1-EH1:1-T2.5	Low	1	1:1:2.5	66.56	2.47	0.80	14.81	0.02	15.60
6	US3-EH1:1-T2.5	Low	3	1:1:2.5	66.68	2.32	0.83	15.43	0.02	15.30
7	US0.5-EH1:1-T2.5	High	0.5	1:1:2.5	65.11	2.54	0.51	20.08	0.02	13.63
8	US1-EH1:1-T2.5	High	1	1:1:2.5	64.95	2.40	0.63	19.56	0.02	14.63
9	US3-EH1:1-T2.5	High	3	1:1:2.5	57.75	2.32	0.64	22.81	0.01	20.10
10	US3-EH1:0.75-T10	Low	3	1:0.75:10	63.53	2.26	0.75	14.12	0.02	17.70
11	US3-EH1:1-T10	Low	3	1:1:10	63.18	2.45	0.75	17.95	0.01	16.83
12	US3-EH0.75:1-T10	Low	3	0.75:1:10	67.21	2.29	0.87	14.35	0.01	15.37
13	US3-EH1:1-T15	Low	3	1:1:15	67.71	2.27	1.01	14.26	0.02	14.60

Note: US: Ultrasound; EH: EDC-HOBt; T: TEPA.
Number beside US denotes sonication time in minutes; Number beside EH denotes ratio of activating agents; Number beside T denotes amine loading.

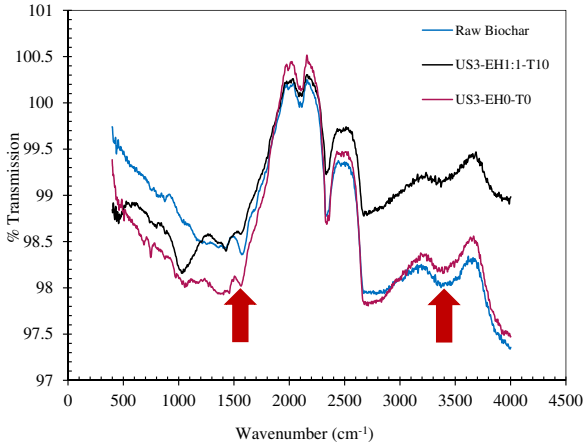

Fig. 4. IR spectrum of Raw Biochar, US3-EH1:1-T10, and US3-EH0-T0.

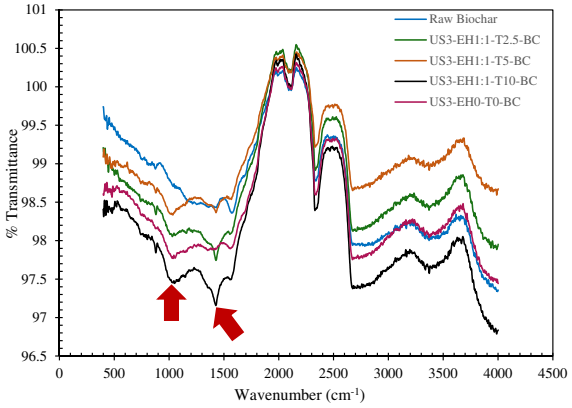

Fig. 5. IR spectrum of Raw Biochar, US3-EH1:1-T2.5, US3-EH1:1-T5, US3-EH1:1-T10, and US3-EH0-T0.

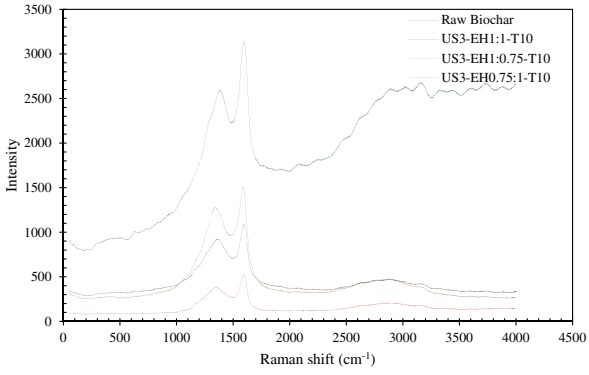

Fig. 6. Raman spectra of Raw Biochar, US3-EH1:1-T10, US3-EH1:0.75-T10, and US3-EH0.75:1-T10.

to 0.75 for 0.75:1. The D peak was higher than G peak in all the spectra which indicates transition from sp^2 to sp^3 material [22]. The I_D/I_G ratio was higher for activated samples than for R, which signifies that the activated samples have more defects on carbon, presumably in the form of oxygen functionality [22]. The maximum departure of the I_D/I_G ratio was found for the 1:1 ratio, suggesting the maximum defects resulting from aminations.

Next in Fig. 7 the Raman spectra for R, US3-EH1:1-T2.5, US3-EH1:1-T5, US3-EH1:1-T10, and US3-EH0-T0 are represented. The D band appeared at 1367 cm^{-1}, 1417 cm^{-1}, 1365 cm^{-1} and 1371 cm^{-1} for

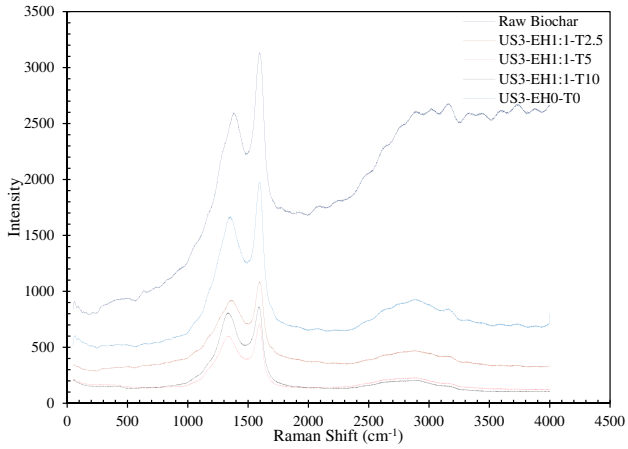

Fig. 7. Raman spectra of Raw Biochar, US3-EH1:1-T2.5, US3-EH1:1-T5, US3-EH1:1-T10, and US3-EH0 T0.

US3-EH1:1-T2.5, US3-EH1:1-T5, US3-EH1:1-T10, and US3-EH0-T0, respectively. The G peak appeared at 1651 cm^{-1}1, 1614 cm^{-1}, 1577 cm^{-1}, and 1602 cm^{-1}. As was discussed earlier, the D peak is associated with nanocrystalline carbon while the G peak corresponds to amorphous carbon materials. The I_D/I_G ratios for US3-EH1:1-T2.5, US3-EH1:1-T5, US3-EH1:1-T10, and US3-EH0-T0 were 0.85, 0.86, 0.87 and 0.83, respectively. This illustrates that more distortion was introduced into biochar surface upon more extensive activation, since the I_D/I_G ratio increased.

Further, the Raman spectra of samples sonicated for different times are shown in Fig. 8. For US0.5-EH1:1-T2.5, US1-EH1:1-T2.5 and US3-EH1:1-T2.5, the D peak was observed at 1382 cm^{-1}, 1355 cm^{-1} and 1374 cm^{-1}; and the G peak appeared at 1606 cm^{-1}, 1608 cm^{-1} and 1611 cm^{-1}, respectively. The I_D/I_G ratios were 0.85, 0.76 and 0.85. This is further evidence that the sonication time of 30 s provided the optimum value of adsorption capacity, since it had the maximum intensity ratio. The values of intensity ratios for all the biochar samples have been summarized in Table 4.

3.3. CO_2 capture study of physico-chemical activated biochar

The adsorption capacity of ultrasound treated-amine functionalized biochar synthesized under different conditions are summarized in Table 5. Firstly, the effect of activating agents was investigated. Experiments were carried out with three different ratios of EDC:HOBt, namely 1:1, 1:0.75 and 0.75:1. The biochar samples activated with 1:1 EDC:HOBt exhibited the highest CO_2 capture capacity. Therefore, this ratio was chosen for all subsequent experiments. Confirmation was also obtained from Raman spectra (Fig. 6), showing the highest I_D/I_G ratio for 1:1 EDC:HOBt, attributed to the greatest conversion of acid functionalities to amide. The requirement for a 1:1 ratio is consistent with the mechanism described in Fig. 3. EDC attaches to the −COOH group in the first step and then HOBt replaces EDC completely to activate the carboxyl group. So, an equal amount of HOBt is required to substitute EDC completely. The second factor which contributed to improving adsorption capacity was amine loading. The amine loading was varied from 2.5 to 15 times the weight of biochar, keeping the activating agents at their optimum ratio. The adsorption capacity of the biochar steadily increased with amine loading up to 10 times weight, and then reduced at 15. Therefore, an amine loading at 10 times the biochar weight was considered as the optimum loading capacity. Additionally, elemental analysis pointed out enhancement in nitrogen content with increasing amine loading. The effect of amine loading can be substantiated from the surface area analysis results. Both DR-CO_2 and BET-N_2 analysis results indicate reductions in surface area due to amine attachment (Table 2). The reasoning behind this trend is that the number of oxygen functional groups on the biochar surface are fixed. Therefore, addition of excess amine would not assure its complete reaction with oxygen functionalities. Rather, excess amine would decrease CO_2 capture because of inaccessible surface area, formed by blocking pores to prevent intercalation of more amines. A similar trend was observed by Zhao et al. [19]. They treated their graphene oxide sample with 10%, 50% and 100% amine loading. Adsorption capacity increased from 10% to 50% loading. But further increase negatively affected the adsorption capacity. In this study, the nitrogen content increases with amine loading, as seen from the elemental analysis.

From Table 5, it can be observed that the adsorption capacity increases gradually as the activating agent ratio and amine loading are optimized. But additional improvement was observed when the duration of sonication was optimized. In fact, ultrasound irradiation had a predominant effect in improving CO_2 capture capacity. Biochar-water mixtures were exposed to ultrasound irradiation times of 30 s, 1 min and 3 min. From no ultrasonication time to 30 s the adsorption capacity enhanced, but longer sonication times reduced the capture capacity. Similar results obtained with either low-energy or high-energy ultrasound. As sonication time progresses, the temperature of the biochar-water mixture increases. Consequently, the surface tension of the medium decreases and vapor pressure inside the microbubbles increases; this in turn reduces shock waves [20]. This foils the formation and collapse of microbubbles and reduces sonication efficiency. Thus, the adsorption capacity reduced. The results are also consistent with the surface area analysis where micropore surface area reduced as sonication time increased. For 60 s of sonication, the micropore surface area reduced from 354 m^2/g to 268.8 m^2/g. However, 30 s of sonication significantly increased the adsorption capacity of the modified biochar compared with samples functionalized without ultrasound. This can be explained based on the mass transport phenomena mentioned earlier. The mass transport inside the pores was expedited by ultrasound due to increased turbulence caused by sonication. Advantages of sonication as a physical activation technique include its use at ambient temperature and its very short time requirement.

3.3.1. Effect of temperature

Adsorption experiments were carried out at different temperatures ranging from 25 °C to 90 °C (Table 5). The results indicated a gradual increase in adsorption capacity with temperature up to 70 °C, while a higher temperature negatively affected CO_2 adsorption. At the optimum temperature, 70 °C, the adsorptive capacity was 63% higher than at room temperature (25 °C). Following amine activation, the main adsorption process is expected to be chemisorption. Chemisorption

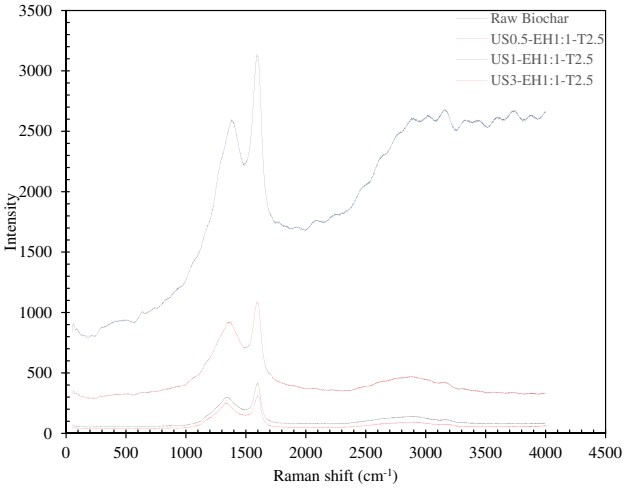

Fig. 8. Raman spectra of Raw Biochar, US0.5-EH1:1-T2.5, US1-EH1:1-T2.5, and US3-EH1:1-T2.5.

Table 4
Summary of intensity ratio for raw biochar and ultrasonicated amine functionalized biochar samples.

Sample name	Intensity ratio value
Raw biochar	0.82
US3-EH1:1-T10	0.87
US3-EH0.75:1-T10	0.75
US3-EH1:0.75-T10	0.85
US3-EH1:1-T2.5	0.85
US3-EH1:1-T5	0.86
US3-EH0-T0	0.83
US0.5-EH1:1-T2.5	0.85
US1-EH1:1-T2.5	0.76

Note: US: Ultrasound; EH: EDC-HOBt; T: TEPA.
Number beside US denotes sonication time in minutes; Number beside EH denotes ratio of activating agents; Number beside denotes amine loading.

Table 5
Effect of process parameters on CO_2 adsorption capacity.

Sample name	Adsorption capacity (mmol/g)	Temp. (°C)	CO_2 conc. (vol%)
Raw biochar			
Raw biochar	0.3	70	10
Low energy ultrasound	*Effect of Activating agents*		
US3-EH1:0.75-T10	0.61	70	10
US3-EH1:1-T10	0.67	70	10
US3-EH0.75:1-T10	0.59	70	10
Low energy ultrasound	*Effect of amine concentration*		
US3-EH0-T0	0.55	70	10
US3-EH1:1-T2.5	0.69	70	10
US3-EH1:1-T5	0.72	70	10
US3-EH1:1-T10	0.75	70	10
US3-EH1:1-T15	0.70	70	10
Effect of ultrasound *Low energy ultrasound*			10
US0-EH1:1-T2.5	0.56	70	10
US0.5-EH1:1-T2.5	1.69	70	10
US1-EH1:1-T2.5	0.78	70	10
US3-EH1:1-T2.5	0.69	70	10
High energy ultrasound			
US0-EH1:1-T2.5	0.55	70	10
US0.5-EH1:1-T2.5	2.04	70	10
US1-EH1:1-T2.5	1.73	70	10
US3-EH1:1-T2.5	1.58	70	10
High energy ultrasound	*Effect of temperature*		
US0.5-EH1:1-T2.5-25°	1.32	25	10
US0.5-EH1:1-T2.5-50°	1.48	50	10
US0.5-EH 1:1-T2.5-70°	2.04	70	10
US0.5-EH 1:1-T2.5-90°	1.10	90	10
High energy ultrasound	*Effect of CO_2 concentration (vol%)*		
US0.5-EH 1:1-T2.5-70°-C10	2.04	70	10
US0.5-EH1:1-T2.5-70°-C13	2.31	70	13
US0.5-EH 1:1-T2.5-70°-C15	2.79	70	15

Note: C-inlet CO_2 concentration.
Number beside C denotes inlet CO_2 concentration in vol%.

involves a higher activation energy than physisorption. Hence, the initial increase of adsorption capacity with temperature is due to the higher activation energy requirement of chemisorption. But later it reduced due to exothermic nature of adsorption [24]. A similar phenomenon was observed by Heydari-Gorji et al. [24] where CO_2 uptake was favored at a higher temperature (75 °C) than at a lower temperature (25 °C) for polyethyleneimine (PEI) supported on mesoporous silica. Similarly, a study by Jadhav et al. [25] demonstrated that CO_2 adsorption by monoethanolamine (MEA) modified Zeolite 13X was favored at a higher temperature (120 °C) than at a lower temperature (30 °C). They explained this behavior using diffusion theory and demonstrated the dispersion state of amine within the porous system of their adsorbent mesoporous silica.

3.3.2. *Effect of CO_2 concentration*

Inlet CO_2 concentration is a driving force for improving CO_2 capture capacity. To determine the effect of inlet CO_2 concentration on adsorption capacity, experiments were carried out with different concentrations of CO_2. Usually, flue gas from power plants contains 10–15 vol% of CO_2. Accordingly and in order to determine the effect of CO_2 concentration on the adsorption capacity of the modified biochar, 10, 13 and 15 vol% of inlet CO_2 concentrations were selected in this study [26,27]. The adsorption capacity increased with the CO_2 concentration in inlet flow (Table 5). The optimum capacity was achieved for 15% inlet CO_2 with the value of 2.79 mmol/g. The diffusion theory can explain this well. When inlet concentration increases, the diffusion velocity of adsorbate increases through the pores of the adsorbent, thus enhancing the resulting adsorption capacity. A similar trend was observed by Shiue et al. [28], where increasing CO_2 concentrations from 800 to 1200 ppm led to increases in CO_2 adsorption capacity from 2.1 to 2.77 mmol/g.

To further depict the efficacy of ultrasonication and amine functionalization on adsorption capacity, a CO_2 adsorption–desorption experiment of ultrasonicated amine-functionalized biochar was conducted and the respective isotherm is shown in Fig. 9. The shape of the isotherm represents the mechanism of adsorption [29]. In this study, the modified adsorbent exhibits a curved isotherm. This is attributed to micropore filling of the adsorbent (during DR micro-porosity analysis) that is in accordance with the surface area analysis (Table 2). Additionally, the desorption branch does not show any hysteresis loop thus, the desorption seems to be partially reversible [30]. The values of adsorption capacity of raw biochar and both low-energy and high-energy ultrasound-irradiated amine-functionalized biochars obtained in the present study are compared with commonly available adsorbents found in the literature in Table 6. The comparison indicates that the adsorption capacity of the modified biochar in our present study is within a very good range, considering that, for most of the sorbents, the maximum capacity was reached with pure CO_2 gas, whereas we used a CO_2-He gas-mixture with only 10– 15% CO_2. Also, the activation for the

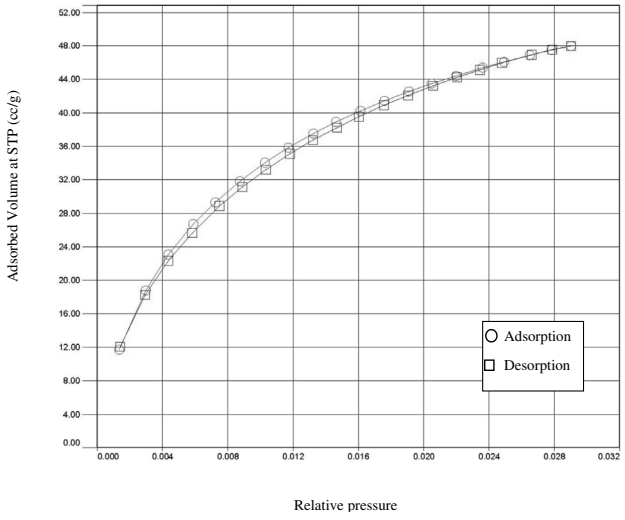

Fig. 9. CO_2 adsorption desorption isotherm of ultrasonicated amine modified biochar at 0 °C.

Table 6
Comparison of present adsorption capacity with literature.

Adsorbent	Capacity (mmol/g)	Activating agent	Activation condition	Adsorption temp (°C)	CO_2%	Ref.
Hickory wood biochar	1.67	–	–	25	100	[3]
Perilla biochar	2.31	–	–	50	40	[36]
Saw dust biochar	1.02	MEA	Room temp	30	100	[37]
Pig manure biochar	0.78	–	–	25	100	[38]
Rubber wood biochar	0.40	–	–	25	100	[39]
PEI on mesoporous carbon	4.82	KOH	700 °C, 0.1 MPa	75	15	[35]
Aminated graphene oxide	1.10	EDA, DETA, TETA	80 °C	30	100	[19]
Fly carbon	1.56	DETA, PEHA, PEI	60 °C, 300 mbar	30	100	[40]
KOH modified activated carbon	4.54	KOH	800 °C	25	100	[41]
Commercial carbon molecular sieve	4.06	Acetylene	600–900 °C	25	30	[42]
Pine wood biochar (raw)	0.30	–	–	70	10	Present study
Pine wood biochar[1]	1.69	TEPA	Room temp	70	10	Present study
Pine wood biochar[2]	2.04	TEPA	Room temp	70	10	Present study
Pine wood biochar[2]	2.79	TEPA	Room temp	70	15	Present study

Note: [1]Low energy ultrasound system, [2] High energy ultrasound system.

present study takes place at room temperature with only 30 s of ultrasonic exposure. On the contrary, many of the traditional activation techniques require very high temperature, usually above 700 °C. Therefore, this study proved to be an effective technique of functionalizing biochar, utilizing a minimum energy from ultrasonic irradiation and a moderate quantity of amine, and still providing a high adsorption capacity – higher than any other biochar in Table 6. To improve the adsorption capacity further, the present work will be extended using different amine and dual amine techniques to attain a maximum CO_2 adsorption capacity.

3.4. Cyclic adsorption-regeneration of adsorbent

Regeneration of adsorbent is necessary from an economic point of view and for long term use. A regeneration experiment was conducted by heating the adsorbent (US0.5-EH1:1-T2.5) at the elevated temperature of 180 °C under helium (He) gas flow for 60 min. The adsorbent after regeneration was reused in the CO_2 adsorption experiment. After 15 cycles of adsorption-regeneration, the adsorptive capacity was reduced by 44% as shown in Fig. 10.

Regeneration processes are usually applied at very high temperatures, ranging from 200 to 500 °C [31,32]. However, in the present study, 180 °C was used to make the process less energy intensive and more economic. Higher temperature ascertains a better desorption rate but at the expense of high energy. Moreover, the desorption behavior of the prepared adsorbent can be further enhanced by employing a suitable catalyst that improves the regeneration ability at a low desorption temperature which is a focus of our coming works.

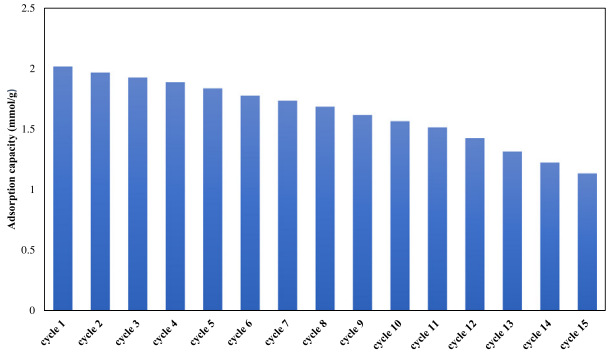

Fig. 10. Cyclic adsorption-desorption behavior of sonicated-TEPA-modified biochar.

4. Conclusions

The current study aimed at introducing a fast, economically feasible and efficient physico-chemical method for the modification of biochar. In this process, biochar was first treated under ultrasonic irradiation with an optimum exposure time of only 30 s, followed by chemical amination at room temperature. From the characterization of activated biochar, it became clear that ultrasound exfoliated the graphene clusters of biochar, cleaned and opened blocked micro-pores, and increased its surface area. All these factors intensified the chemical functionalization of biochar with TEPA. The ultrasound-treated, amine-modified biochar was then used for adsorption of CO_2. The interaction between the nucleophilic active sites on the modified biochar surface and the electrophilic CO_2 molecules facilitated adsorption through the formation of covalent bonding. The present study revealed that the combination of a physical activation method with chemical amine modification can lead to a very high adsorption capacity. Raw biochar had a very limited adsorption capacity of 0.3 mmol/g, but its capacity increased to 2.79 mmol/g (at 70 °C with 0.15 atm partial CO_2 pressure and 15 vol% inlet CO_2) after both physical modification with low frequency ultrasound and chemical activation with amine (TEPA). The adsorption capacity of physico-chemical activated biochar was over 9 times that of raw biochar. In addition, the adsorbent was underwent in a cyclic adsorption-regeneration experiment, which revealed that the adsorption capacity after 15 cycles retained 56% of the initial adsorption capacity. Aside from the promising results obtained in terms of CO_2 adsorption, the developed ultrasonic treatment process was very efficient in terms of energy and time. Biochar was exposed to ultrasound irradiation for only 30 s at room temperature. Moreover, amine functionalization of ultrasono-treated biochar was accomplished with little warming at 35 °C. Hence, the technique applied for modifying biochar proved very efficient, and the produced biochar is a potential sorbent for CO_2 adsorption.

Acknowledgements

The authors are grateful to the National Science Foundation (NSF EPSCoR RII Grant No. OIA-1632899) for financial support. Various other supports from the University of Mississippi are also gratefully acknowledged. Also, the authors would like to acknowledge Dr. Vijayshankar Raman (Pharmacy Department, University of Mississippi) and Cameron Smith (Department of Chemistry and Biochemistry, University of Mississippi) for helping in SEM and Raman analysis, respectively.

Appendix A. Supplementary data

Supplementary data associated with this article can be found, in the online version, at http://dx.doi.org/10.1016/j.fuel.2018.03.145.

References

[1] Yu C-H, Huang C-H, Tan C-S. A review of CO_2 capture by absorption and adsorption. Aerosol Air Qual Res 2012;12(5):745–69.
[2] Choi S, Drese JH, Jones CW. Adsorbent materials for carbon dioxide capture from large anthropogenic point sources. ChemSusChem 2009;2(9):796–854.
[3] Creamer AE, Gao B, Zhang M. Carbon dioxide capture using biochar produced from sugarcane bagasse and hickory wood. Chem Eng J 2014;249:174–9.
[4] Cubas SA, Foresti E, Rodrigues JAD, Ratusznei SM, Zaiat M. Effect of impeller type and stirring frequency on the behavior of an AnSBBR in the treatment of low-strength wastewater. Bioresour Technol 2011;102(2):889–93.
[5] Zimmerman AR. Abiotic and Microbial Oxidation of Laboratory-Produced Black Carbon (Biochar). Environ Sci Technol 2010;44(4):1295–301.
[6] Chen WY, Mattern DL, Okinedo E, Senter JC, Mattei AA, Redwine CW. Photochemical and acoustic interactions of biochar with CO_2 and H_2O: applications in power generation and CO_2 capture. AIChE J 2014;60(3):1054–65.
[7] Aslanzadeh S, Rajendran K, Taherzadeh MJ. A comparative study between single- and two-stage anaerobic digestion processes: effects of organic loading rate and hydraulic retention time. Int Biodeterior Biodegrad 2014;95(Part A):181–8.
[8] Adelodun AA, Kim K-H, Ngila JC, Szulejko J. A review on the effect of amination pretreatment for the selective separation of CO_2. Appl Energy 2015;158:631–42.
[9] Chateauneuf JE, Zhang J, Foote J, Brink J, Perkovic MW. Photochemical fixation of supercritical carbon dioxide: the production of a carboxylic acid from a polyaromatic hydrocarbon. Adv Environ Res 2002;6(4):487–93.
[10] Park S, An J, Jung I, Piner RD, An SJ, Li X, et al. Colloidal suspensions of highly reduced graphene oxide in a wide variety of organic solvents. Nano Lett 2009;9(4):1593–7.
[11] Verma YL, Singh MP, Singh RK. Effect of ultrasonic irradiation on preparation and properties of ionogels. J Nanomater 2012;2012:6.
[12] Hamdaoui O, Naffrechoux E, Tifouti L, Pétrier C. Effects of ultrasound on adsorption–desorption of p-chlorophenol on granular activated carbon. Ultrason Sonochem 2003;10(2):109–14.
[13] Levêque J-M, Duclaux L, Rouzaud J-N, Reinert L, Komatsu N, Desforges A, et al. Ultrasonic treatment of glassy carbon for nanoparticle preparation. Ultrason Sonochem 2017;35:615–22.
[14] Stankovich S, Dikin DA, Dommett GHB, Kohlhaas KM, Zimney EJ, Stach EA, et al. Graphene-based composite materials. Nature 2006;442(7100):282–6.
[15] Lin Z, Karthik PS, Hada M, Nishikawa T, Hayashi Y. Simple technique of exfoliation and dispersion of multilayer graphene from natural graphite by ozone-assisted sonication. Nanomaterials 2017;7(6):125.
[16] Al-Warhi TI, Al-Hazimi HMA, El-Faham A. Recent development in peptide coupling reagents. J Saudi Chem Soc 2012;16(2):97–116.
[17] Koenig W, Geiger R. A new method for synthesis of peptides: activation of the carboxyl group with dicyclohexylcarbodiimide using 1-hydroxybenzotriazoles as additives. Chemische Berichte 1970;103(3):788.
[18] Montalbetti CA, Falque V. Amide bond formation and peptide coupling. Tetrahedron 2005;61(46):10827–52.
[19] Zhao Y, Ding H, Zhong Q. Preparation and characterization of aminated graphite oxide for CO_2 capture. Appl Surf Sci 2012;258(10):4301–7.
[20] Berto DA, Hauptli L, Saleh MA, Padilha PM. The ultra-sonication of minerals in swine feed. J Anim Sci Biotechnol 2015;6(1):32.
[21] Biswal D, Singh R. Characterisation of carboxymethyl cellulose and polyacrylamide graft copolymer. Carbohydr Polym 2004;57(4):379–87.
[22] Ferrari AC. Raman spectroscopy of graphene and graphite: disorder, electron–phonon coupling, doping and nonadiabatic effects. Solid State Commun 2007;143(1):47–57.
[23] Perumbilavil S, Sankar P, Priya Rose T, Philip R. White light Z-scan measurements of ultrafast optical nonlinearity in reduced graphene oxide nanosheets in the 400–700 nm region. Appl Phys Lett 2015;107(5):051104.
[24] Heydari-Gorji A, Belmabkhout Y, Sayari A. Polyethylenimine-impregnated mesoporous silica: effect of amine loading and surface alkyl chains on CO_2 adsorption. Langmuir 2011;27(20):12411–6.
[25] Jadhav P, Chatti R, Biniwale R, Labhsetwar N, Devotta S, Rayalu S. Monoethanol amine modified zeolite 13X for CO_2 adsorption at different temperatures. Energy Fuels 2007;21(6):3555–9.
[26] Sean I. Review of CO_2 capture technologies and some improvement opportunities.
[27] Songolzadeh M, Soleimani M, Takht Ravanchi M, Songolzadeh R. Carbon dioxide separation from flue gases: a technological review emphasizing reduction in greenhouse gas emissions. Sci World J 2014;2014.
[28] Shiue A, Hu S-C, Chang S-M, Ko T-Y, Hsieh A, Chan A. Adsorption kinetics and breakthrough of carbon dioxide for the chemical modified activated carbon filter used in the building. Sustainability 2017;9(9):1533.
[29] Foo KY, Hameed BH. Insights into the modeling of adsorption isotherm systems. Chem Eng J 2010;156(1):2–10.
[30] Chaffee AL, Knowles GP, Liang Z, Zhang J, Xiao P, Webley PA. CO2 capture by adsorption: materials and process development. Int J Greenhouse Gas Control 2007;1(1):11–8.
[31] Song X, Li K, Wang C, Sun X, Ning P, Tang L. Regeneration performance and mechanism of modified walnut shell biochar catalyst for low temperature catalytic hydrolysis of organic sulfur. Chem Eng J 2017;330:727–35.
[32] Lashaki MJ, Fayaz M, Wang H, Hashisho Z, Philips JH, Anderson JE, et al. Effect of adsorption and regeneration temperature on irreversible adsorption of organic vapors on beaded activated carbon. Environ Sci Technol 2012;46(7):4083–90.
[33] Keskes E, Adjiman CS, Galindo A. A physical absorption process for the capture of CO_2 from CO_2-rich natural gas streams; 2006.
[34] Spigarelli BP, Kawatra SK. Opportunities and challenges in carbon dioxide capture. J CO_2 Util 2013;1:69–87.
[35] Hinkov I, Lamari FD, Langlois P, Dicko M, Chilev C, Pentchev I. Carbon dioxide capture by adsorption. J Chem Technol Metall 2016;51(6).
[36] Sethupathi S, Zhang M, Rajapaksha AU, Lee SR, Mohamad Nor N, Mohamed AR, et al. Biochars as potential adsorbers of CH_4, CO_2 and H_2S. Sustainability 2017;9(1):121.
[37] Madzaki H, KarimGhani WAWA. Carbon dioxide adsorption on sawdust biochar. Procedia Eng 2016;148:718–25.
[38] Xu X, Kan Y, Zhao L, Cao X. Chemical transformation of CO_2 during its capture by waste biomass derived biochars. Environ Pollut 2016;213(Suppl. C):533–40.
[39] Ghani WAWAK, Mohd A, da Silva G, Bachmann RT, Taufiq-Yap YH, Rashid U, et al. Biochar production from waste rubber-wood-sawdust and its potential use in C sequestration: chemical and physical characterization. Ind Crops Prod 2013;44:18–24.
[40] Plaza M, Pevida C, Arenillas A, Rubiera F, Pis J. CO_2 capture by adsorption with nitrogen enriched carbons. Fuel 2007;86(14):2204–12.
[41] Sreńscek-Nazzal J, Narkiewicz U, Morawski AW, Wróbel RJ, Michalkiewicz B. The increase of the micoporosity and CO_2 adsorption capacity of the commercial activated carbon CWZ-22 by KOH treatment. In: Dariani RS, editor. Microporous and mesoporous materials. Rijeka: InTech; 2016, p. Ch. 01.
[42] Anuwattana R, Patkool C, Chawakitchareon P. Carbon dioxide adsorption using activated carbon via chemical vapor deposition process. Eng J 2016;20(4).